Robust GNSS phase tracking in case of slow dynamics using variational Bayes inference

Fabio Fabozzi, Stéphanie Bidon, Sébastien Roche, Benoit Priot

Robust GNSS phase tracking in case of slow dynamics using variational Bayes inference

Fabio Fabozzi*, Stéphanie Bidon*, Sébastien Roche† and Benoît Priot*
*ISAE-SUPAERO, Université de Toulouse, France
Email: {fabio.fabozzi,stephanie.bidon,benoit.priot}@isae-supaero.fr
†Airbus Defence and Space, Toulouse, France
Email: sebastien.roche@airbus.com

***Abstract*—For a precise GNSS (Global Navigation Satellite System) positioning, carrier phase measurements are required. However, cycle slipping in classical phase locked loop (PLL) can lead to a local or permanent loss of lock. To address this problem, we propose a robust nonlinear filter for carrier phase tracking based on Variational Bayes (VB) inference. So far, the algorithm is designed only for slow phase dynamics (i.e., first order loop). Interestingly, the estimator update equation can be expressed in closed form. Performance of our algorithm is assessed on synthetic and experimental GNSS data and compared to that of conventional PLL-based techniques. Results show that the proposed method brings significant improvement in terms of cycle slipping.**

***Index Terms*—Phase tracking, Cycle slips, Nonlinear Bayesian filtering, Variational Bayes approximation**

I. Introduction

Precise GNSS positioning is crucial in a wide range of applications (e.g., surveying [1]). Carrier-based techniques such as Real-Time Kinematic (RTK) and Precise Point Positioning (PPP) have been accordingly developed [2]. They can provide positions that are orders of magnitude more accurate than code-based GNSS [3]. However, phase measurements obtained by conventional phase tracking algorithms can be severely impaired by the presence of ambiguous phase jumps known as cycle slips. They particularly arise in degraded environments. These local losses of lock can even lead the tracking loop to a complete drop-lock from which it never recovers. Reacquisition is then necessary which severely afflicts the positioning efficiency. Cycle slip phenomenon has been extensively studied in literature, e.g., [3]–[8]. To guarantee a robust carrier tracking in the presence of singular inputs or harsh environmental conditions, different techniques have been developed [9].

In this paper, we propose a nonlinear filtering technique for robust GNSS phase tracking based on the VB approximation [10]. This study is the continuation of the work presented in [11] where a VB-based phase tracking technique was developed for correlated bi-frequency measurements. Herein, we consider instead a conventional mono-frequency GNSS channel and show that the signal model allows the same tracking methodology to be applied. Particularly, unlike conventional PLL-based techniques, no linear approximation is made about the phase measurement which is a distinct advantage especially at low signal-to-noise-ratio (SNR). We thus obtain a closed-form nonlinear update equation that is simple to implement. Our work is so far limited to slow phase dynamics.

The paper is organized as follows. Section II describes the scenario into the GNSS framework and the signal model considered. The variational Bayes approximation is recalled and applied accordingly in Section III. Numerical results are then presented in Section IV. Conclusions are summarized in the last section.

The work of Fabio Fabozzi is supported by the DGA (Direction Générale de l'Armemement) under grant 2018 60 0014 and by Airbus Defence and Space.

II. Signal model

A. Scenario

We consider a GNSS receiver with a scalar tracking architecture, i.e., the signal received is processed independently on a satellite basis and that for each available frequency channel. The proposed phase tracking algorithm is developed assuming that either delay or both delay and frequency are perfectly synchronized after the satellite acquisition stage. Actually, this assumption could be related to two possible receiver's architecture:

1) the tracking block entails only a Delay Lock Loop (DLL) and the frequency is compensated with that estimated at the acquisition stage; this architecture is realistic only during a certain amount of time since an integration loss will appear due to a non-tracked frequency;
2) the tracking block entails both a DLL-FLL (Frequency Lock Loop).

In both cases, the proposed phase tracking technique estimates the (residual) phase of the prompt. In addition, no feedback of the estimated phase is provided to the DLL. In this study, results provided on real data are obtained with the former architecture.

B. Measurement model

We consider the prompt signal as described in Section II-A while assuming that both delay and frequency are perfectly synchronized. The resulting baseband signal at the instant k can be expressed as

$$z_k = \alpha e^{j\phi_k} + n_k \tag{1}$$

where α is the real amplitude on receive, ϕ_k is the remaining phase to be tracked and n_k is the internal receiver noise. In (1), it is also assumed that there is no navigation message (i.e., either a pilot channel is considered or data wipe-off is applied)

1) Likehood function: The noise component n_k is supposed to be complex white and Gaussian with known power σ_n^2, hence

$$n_k \sim \mathcal{CN}(0, \sigma_n^2). \tag{2}$$

Using (1) and (2), the likelihood function can be expressed as

$$\begin{aligned} f(z_k|\phi_k, \alpha, \sigma_n^2) &= \frac{1}{\pi\sigma_n^2}\exp\Big\{-\frac{|z_k - \alpha e^{j\phi_k}|^2}{\sigma_n^2}\Big\} \\ &= \frac{1}{\pi\sigma_n^2}\exp\Big\{-\frac{1}{\sigma_n^2}\Big[|z_k|^2 + \alpha^2 - 2\alpha|z_k|\cos(\phi_k - \psi_k)\Big]\Big\} \end{aligned} \tag{3}$$

with $\psi_k = \text{atan2}(\Im\{z_k\}, \Re\{z_k\})$ the angle that lies between $[-\pi, \pi]$. In this work, we assume to know the value of the amplitude α and noise power σ_n^2 from a lock estimator, we will thus omit them from the conditional terms. Accordingly, the likelihood function (3) can be simply written $f(z_k|\phi_k)$. The sensor factor associated to the likelihood (3) is

$$S(\phi_k) \overset{\text{def}}{=} f(z_k|\phi_k) \propto \exp\Big\{\beta_k \cos(\phi_k - \psi_k)\Big\} \tag{4}$$

where

$$\beta_k = \frac{2\alpha|z_k|}{\sigma_n^2}. \tag{5}$$

In (4), we recognize a Von Mises distribution with concentration parameter β_k and mean direction ψ_k. Considering (1), β_k is distributed according to a Rice distribution with probability density function (pdf) [12]

$$f\Big(\beta_k|m, \frac{\sigma_n^2}{2}\Big) = \frac{2\beta_k}{\sigma_n^2}\exp\Big(\frac{-(\beta_k^2 + m^2)}{\sigma_n^2}\Big) I_0\Big(\frac{2\beta_k m}{\sigma_n^2}\Big) \tag{6}$$

where $m = \alpha$ and I_0 is the modified Bessel function of first kind at zeroth order.

C. Phase process

The phase evolution is modeled by a Markov Random Field (MRF). The latter has been widely used as Bayesian prior in many phase processing problems; [13]–[15] are just few of them. In this study, a first order Gaussian MRF is chosen in order to ensure some smoothness in the estimated phase sequence [14], i.e.,

$$\phi_k = \phi_{k-1} + w_k \tag{7}$$

where $w_k \sim \mathcal{N}(0, \sigma_\phi^2)$ is a white Gaussian noise. The initial state ϕ_1 is supposed to be uniformly distributed over the set $\mathcal{I} = [-\pi, \pi]$. The a priori phase dynamics model can thus be summarized by

$$f(\phi_1) \propto \mathbb{I}_{[-\pi,\pi]}(\phi_1) \tag{8a}$$

$$f(\phi_k|\phi_{k-1}, \sigma_\phi^2) = \frac{1}{\sqrt{2\pi\sigma_\phi^2}}\exp\left\{-\frac{[\phi_k - \phi_{k-1}]^2}{2\sigma_\phi^2}\right\}. \tag{8b}$$

III. Variational Bayes tracking algorithm

Herein, as discussed in the Introduction, the Restricted Variational Bayesian (RVB) approximation is used in the phase tracking problem. The methodology is actually the same as that presented in [11].

A. Distributional approximations in Bayes filtering problem

The problem of inferring the state variable is described by

$$f(z_k|\phi_k) \quad \text{and} \quad f(\phi_k|\phi_{k-1}).$$

Let denote by $\boldsymbol{Z}_k = [z_1, \ldots, z_k]$ the set of observations till the instant k. The optimal Bayes filtering that evaluates iteratively the filtering distribution $f(\phi_k|\boldsymbol{Z}_k)$ is obtained by alternating between the two following equations

$$\begin{aligned} f(\phi_k|\boldsymbol{Z}_{k-1}) &= f(\phi_1) \qquad k = 1 \\ f(\phi_k|\boldsymbol{Z}_{k-1}) &= \int f(\phi_k|\phi_{k-1}) f(\phi_{k-1}|\boldsymbol{Z}_{k-1}) d\phi_{k-1} \quad k > 1 \end{aligned} \tag{9}$$

and

$$f(\phi_k|\boldsymbol{Z}_k) \propto f(\boldsymbol{z}_k|\phi_k) f(\phi_k|\boldsymbol{Z}_{k-1}) \qquad k > 1. \tag{10}$$

Though, to make the Bayesian filtering tractable and thus guarantee the iteration of its procedure, we will enforce the functional form of the marginal distribution $f(\phi_k|\boldsymbol{Z}_k)$ to remain unchanged along the iteration. A typical way to proceed is to use distribution approximation [16]

$$f(\phi_k|\boldsymbol{Z}_k) \sim \tilde{f}(\phi_k|\boldsymbol{Z}_k). \tag{11}$$

In this study, we focus our attention on the RVB approximation [10].

B. Local Variational Bayesian filtering

The RVB method is based on two approximations applied during the optimal filtering procedure. The first one consists in locally imposing conditional independence between ϕ_k and ϕ_{k-1} [10]

$$\tilde{f}(\phi_k, \phi_{k-1}|\boldsymbol{Z}_k) = \tilde{f}(\phi_k|\boldsymbol{Z}_k)\tilde{f}(\phi_{k-1}|\boldsymbol{Z}_k) \tag{12}$$

where $\tilde{f}(\cdot)$ refers to the approximated posterior distribution. The latter are then chosen to minimize the Kullback Leibler (KL) divergence [10]; the prediction distribution can therefore be expressed as

$$\tilde{f}(\phi_k|\boldsymbol{Z}_{k-1}) \propto \exp\Big(\mathrm{E}_{\tilde{f}(\phi_{k-1}|\boldsymbol{Z}_k)}\Big[\ln(f(\phi_k|\phi_{k-1}))\Big]\Big) \tag{13}$$

with

$$\begin{aligned} \tilde{f}(\phi_{k-1}|\boldsymbol{Z}_k) \propto &\exp\Big(\mathrm{E}_{\tilde{f}(\phi_k|\boldsymbol{Z}_k)}\Big[\ln(f(\phi_k|\phi_{k-1}))\Big]\Big) \\ &\times \tilde{f}(\phi_{k-1}|\boldsymbol{Z}_{k-1}) \end{aligned} \tag{14}$$

where $\mathrm{E}_{\tilde{f}(\boldsymbol{x}_{/i}|\boldsymbol{Z})}\Big[g(\boldsymbol{x})\Big]$ [1] denotes the expected value of the function $g(\boldsymbol{x})$ with respect to the function $f(\boldsymbol{x})$. Accordingly, the filtering distribution is now expressed as

$$\tilde{f}(\phi_k|\boldsymbol{Z}_k) \propto f(\boldsymbol{z}_k|\phi_k)\tilde{f}(\phi_k|\boldsymbol{Z}_{k-1}). \tag{15}$$

[1] $\boldsymbol{x}_{/i}$ denotes the complement of x_i in $\boldsymbol{x}$ (e.g., $\boldsymbol{x}_{/1} = x_2$).

At this stage, the data update equation (15) describes an implicit equation in $\tilde{f}(\phi_k|\boldsymbol{Z}_k)$ since the prediction distribution depends itself via (14) of the latter. To have a closed-form solution, a second approximation is applied [10]. This is done through the *RVB approximation* which finally replaces the distribution $\tilde{f}(\phi_{k-1}|\boldsymbol{Z}_k)$ in (13) by the fixed posterior distribution $\tilde{f}(\phi_{k-1}|\boldsymbol{Z}_{k-1})$. The prediction distribution becomes then

$$\tilde{f}(\phi_k|\boldsymbol{Z}_{k-1}) \propto \exp\Big(\mathrm{E}_{\tilde{f}(\phi_{k-1}|\boldsymbol{Z}_{k-1})}\Big[\ln(f(\phi_k|\phi_{k-1}))\Big]\Big). \tag{16}$$

Using the sensor factor (4) and the phase dynamics distributions (8), it can be shown that, following the same path as in [11], the RVB filtering has the following closed form expression

- Prediction and data update for $k = 1$

$$\tilde{f}(\phi_1|Z_0) \stackrel{\text{def}}{=} f(\phi_1) \tag{17a}$$

$$\tilde{f}(\phi_1|Z_1) \propto f(\phi_1)\exp\Big\{\beta_1\cos(\phi_1-\psi_1)\Big\}. \tag{17b}$$

- Prediction and data update for $k > 1$

$$\phi_k|\boldsymbol{Z}_{k-1} \underset{\tilde{f}}{\sim} \mathcal{N}\Big(\mathrm{E}_{\tilde{f}(\phi_{k-1}|\boldsymbol{Z}_{k-1})}[\phi_{k-1}], \sigma_\phi^2\Big) \tag{18a}$$

$$\tilde{f}(\phi_k|\boldsymbol{Z}_k) \propto \exp\Bigg\{\beta_k\cos(\phi_k-\psi_k) \tag{18b}$$

$$-\frac{\Big[\phi_k - \mathrm{E}_{\tilde{f}(\phi_{k-1}|\boldsymbol{Z}_{k-1})}[\phi_{k-1}]\Big]}{2\sigma_\phi^2}\Bigg\}. \tag{18c}$$

C. Phase tracking estimator

Hence, the RVB approach gives an iterative and tractable solution as long as the approximated posterior mean of ϕ_{k-1} can be evaluated. As in [11], the RVB estimator can be expressed as

- $\hat{\phi}_k^{rvb}$ for $k = 1$

$$\hat{\phi}_1^{rvb} = -2\frac{\sum_{q=1}^{\infty}(-1)^q I_q(\beta_1)\frac{\sin(q\psi_1)}{q}}{I_0(\beta_1)} \tag{19}$$

- $\hat{\phi}_k^{rvb}$ for $k > 1$

$$\hat{\phi}_k^{rvb} = \hat{\phi}_{k-1}^{rvb} + 2\sigma_\phi^2\frac{\sum_{q=1}^{+\infty} qI_q(\beta_k)\sin[q(\psi_k-\hat{\phi}_{k-1}^{rvb})]e^{-\frac{q^2\sigma_\phi^2}{2}}}{I_0(\beta_k)+2\sum_{q=1}^{+\infty} I_q(\beta_k)\cos[q(\psi_k-\hat{\phi}_{k-1}^{rvb})]e^{-\frac{q^2\sigma_\phi^2}{2}}} \tag{20}$$

where the $I_q(\cdot)$'s are the modified Bessel functions of the first kind at qth order. As remarked in [11], since $I_q(\beta_k)$ decreases rapidly with respect to q, an implementable form of (19) and (20) is obtained by truncating the sum involved for $q = 1, ...q_{max}$ where q_{max} is the highest chosen order. Interestingly, the estimate update equation (20) depends non linearly on the innovation term $\psi_k - \phi_{k-1}^{rvb}$.

IV. Numerical simulation

In this section, performance of the proposed RVB estimator (19)-(20) is assessed via synthetic and real GNSS data.

A. Scenario

The received signal is generated as in (1). Considering then an update interval T, the carrier-to-noise-density ratio is defined by

$$C/N_0 = \frac{|\alpha|^2}{\sigma_n^2 T}.$$

In our simulations, the integration time T is chosen equal to 20 ms. The phase dynamics considered are of polynomial form up to the second order, namely

$$\phi_{k+1} = \phi_0 + \dot{\phi}_0 k + \frac{\ddot{\phi}_0 k^2}{2} \tag{21}$$

where ϕ_0, $\dot{\phi}_0$, $\ddot{\phi}_0$ are respectively the initial phase (step), the initial phase rate (ramp) and the initial phase acceleration (parabola). In what follows, the proposed RVB algorithm is compared to a conventional DPLL. Concerning the former, we fix the highest order to $q_{max} = 50$ as proposed in [11]. The value of σ_ϕ is chosen in the interval [0,π] considering that taking a standard deviation greater than half a cycle may favor cycle slip. Concerning the latter and in search of fairness, an ATAN2 discriminator is used and a first order DPLL is considered. Additionally, its phase at initialization $\hat{\phi}_0^{PLL}$ is considered equal to zero and its loop filter coefficient is fixed according to [17]. Therefore the time-bandwidth product $B_L T$ may vary between [0,0.5]. Performance of phase tracking loops is then monitored by statistically studying the phase error process defined as $e_k = \phi_k - \hat{\phi}_k$.

B. Phase tracking from a noise-free observation

First, to better understand the role played by the process noise power σ_ϕ, RVB responses to noise-free signal (i.e., $z_k \stackrel{\text{def}}{=} \alpha e^{j\phi_k}$) are presented in Fig. 1. As could be expected, the proposed first order RVB estimator tracks with no bias a step input, with a finite bias a ramp input (with slow slope) and with an infinite bias an acceleration. Additionally, the parameter σ_ϕ strongly influences the response of the estimator in terms of acquisition time and bias. It thus plays a similar role as that of the loop bandwidth in a conventional DPLL though performance depends nonlinearly on σ_ϕ.

C. Performance metrics

We describe hereafter the performance metrics used to evaluate the RVB estimator (19)-(20). In an attempt to study the tracking algorithm in its linear and nonlinear regimes, we study on the one hand the statistical behavior of the phase error modulo-2π, $\tilde{e}_k = (\phi_k - \hat{\phi}_k)_{[-\pi,\pi]}$ [18], and on the other hand the statistics of the cycle slip event, respectively. More specifically, the following performance metrics are considered.

1) RMSE-mod: To assess the precision of estimation aside cycle slip events, we consider the Root Mean Square Error (RMSE) modulo-2π (denoted as RMSE-mod), i.e.,

$$\text{RMSE-mod} = \sqrt{\mathcal{E}\{\tilde{e}_k^2\}} \stackrel{\text{def}}{=} \sqrt{\frac{1}{M_c}\sum_{n=1}^{M_c}\tilde{e}_k^2(n)}. \tag{22}$$

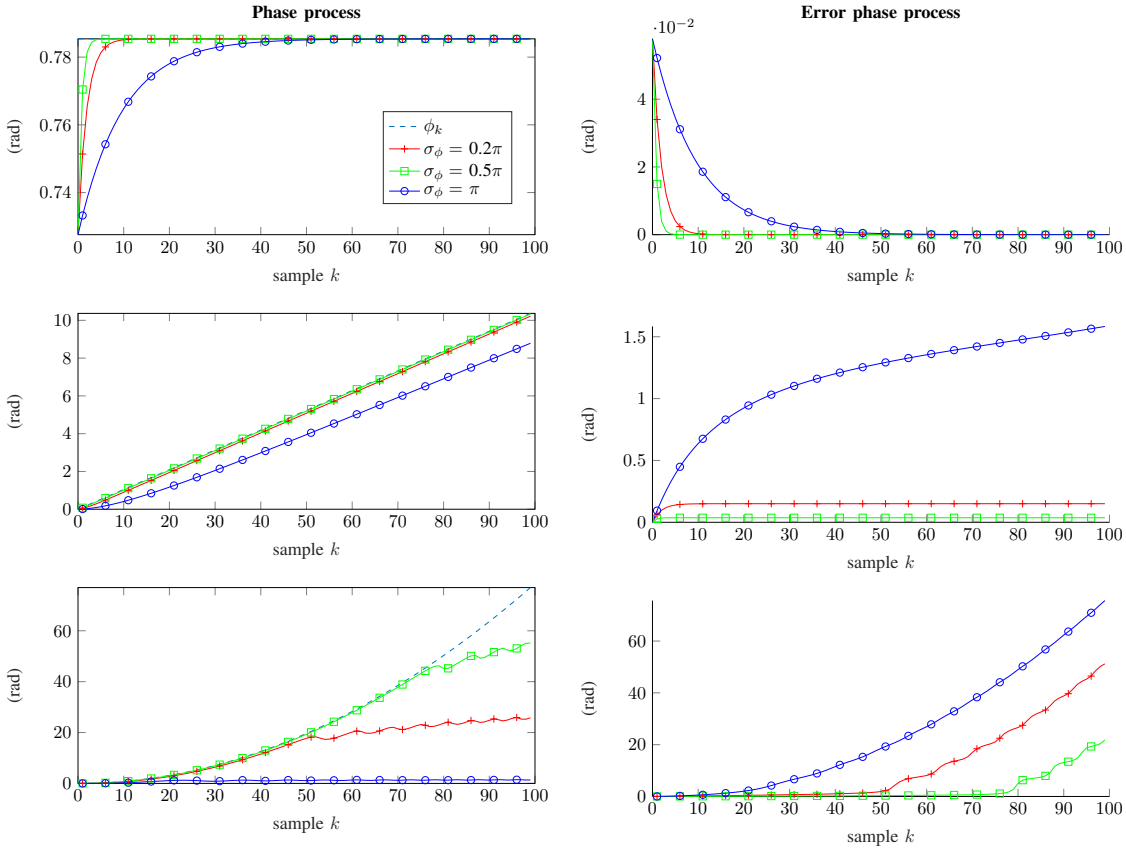

Fig. 1: Phase responses of the RVB estimator to a step- (up), ramp- (middle), and acceleration- (bottom) input: $\phi_0 = \pi/4$ rad; $\dot{\phi}_0 = \pi/30$ rad/sample; $\ddot{\phi}_0 = \pi/(20^2)$ rad/sample^2.

2) Acquisition time: We define it here as the time required for the RMSE-mod to remain constant with respect to the time.

3) Mean time to first cycle slip (or mean time of loss of lock): It is evaluated as the average time required to observe the first cycle slip when the tracking is initialized at steady-state [17]. According to Viterbi's criterion [6], a cycle slip is detected as soon as the phase error crosses a new equilibrium line [6], i.e., when $|e_k^{rvb}| > 2\pi$ since steady-state is initially enforced. Furthermore, the incoming phase is tracked until the first cycle slip occurs. Note that due to the nonlinear nature of the RVB algorithm (20), defining theoretically steady-state is not straightforward. In the simulations, we say that steady-state is reached when the phase error remains constant while assuming a noise-free signal (i.e., $z_k \overset{\text{def}}{=} \alpha e^{j\phi_k}$) and a fixed input phase dynamics. Steady-state is checked and assessed numerically in what follows.

4) Cycle slip rate (or frequency of skipping cycles): It is estimated while fixing a number of cycle slips N_{cs} to be observed. The rate is then estimated as

$$\text{Cycle slip rate} \overset{\text{def}}{=} \frac{1}{M_c} \sum_{n=1}^{M_c} \frac{N_{cs}}{T_{\text{last slip}}(n)}$$

where M_c is the number of Monte-Carlo runs and $T_{\text{last slip}}$ is the time necessary to observe these N_{cs} slips. Also this metrics is evaluated starting the track at steady-state [17].

D. Phase-step response

RMSE-mod of the RVB and DPLL are depicted in Fig. 2 for different standard deviations σ_ϕ and loop bandwidths B_L, respectively. As can be noted, the RMSE-mod reaches a constant value after a given time for each value of σ_ϕ and B_L considered, so that the acquisition time as defined earlier is finite. In Fig. 2, a parametric representation of the RMSE-mod as a function of this acquisition time is given. As is well-known, increasing the DPLL loop bandwidth leads to a faster acquisition (in $\approx 1/(B_L T)$ samples) at the expense of a lower estimation precision. For the RVB, the standard deviation σ_ϕ has a similar influence as that of the loop bandwidth but beyond a given value $\sigma_\phi \approx 0.5\pi$ rad the influence is reversed so that the acquisition time increases while reaching a higher precision. This is due to the nonlinear dependence of the innovation term on σ_ϕ^2 in (20). As a consequence, the same RMSE-mod can be obtained for two different values of σ_ϕ. Additionally, for any fixed acquisition time, the RMSE-mod of the RVB estimator is always lower than that of DPLL. Note also that very low acquisition time can be reached only by the DPLL for very high time-bandwidth product $B_L T$ at the expense of an increased RMSE-mod. Finally, cycle slip rate is depicted in Fig. 4 as a function of σ_ϕ and B_L, respectively.

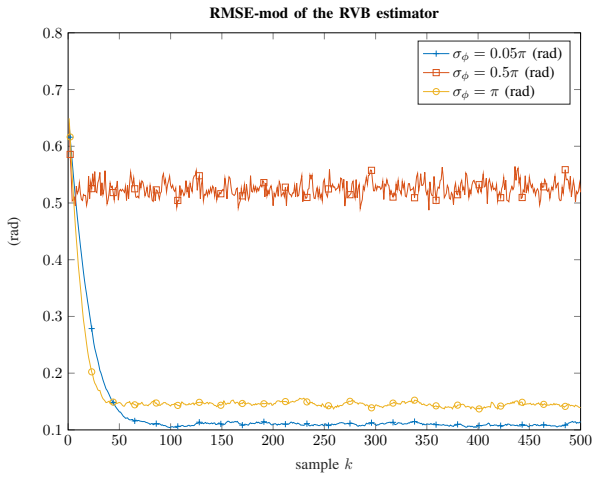

(a) RVB

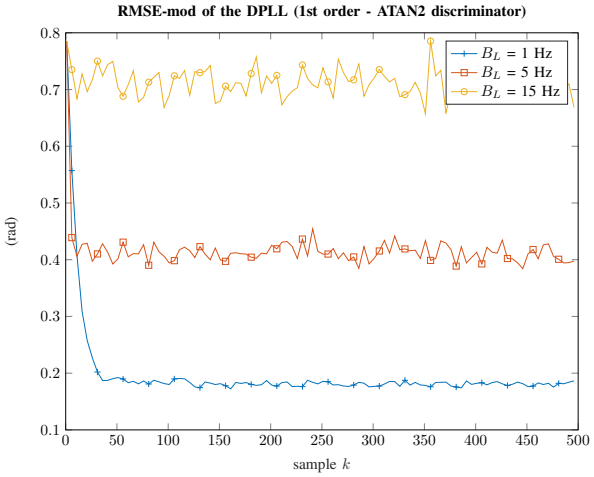

(b) DPLL (1st order - ATAN2 discriminator)

Fig. 2: RMSE-mod as a function of the time index for a step phase input: C/N_0 = 17 dB-Hz; ϕ_0 = π/4 rad; σ_n^2 = 1.

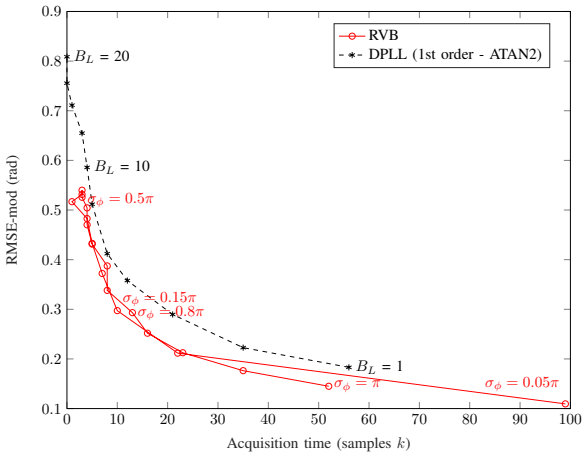

Fig. 3: Precision of estimation metrics comparison for a step phase input: $\phi_0 = \pi/4$ rad; σ_n^2 = 1; C/N_0 = 17 dB-Hz.

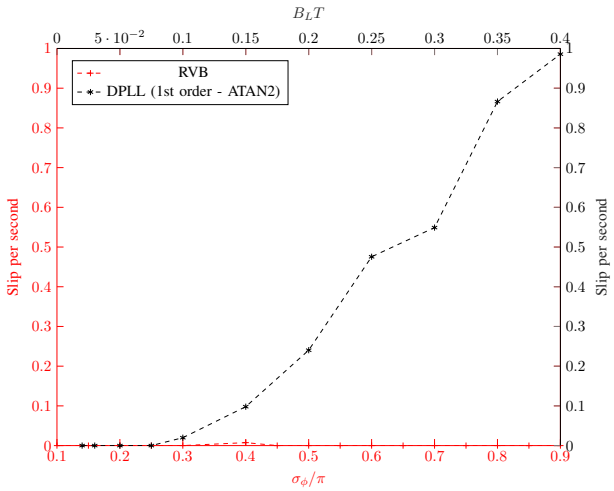

Fig. 4: Cycle slip rate comparison for a step phase input: $\phi_0 = \pi/4$ rad; σ_n^2 = 1; C/N_0 = 15 dB-Hz.

We observe that the RVB algorithm can reach extremely low cycle slip occurrence (around zero slip per second for each σ_ϕ), contrarily to the DPLL. As expected, for the latter the cycle slip rate increases with the loop bandwidth B_L. Note that, in practice, if after a very long time of simulation no cycle slip occurs, we set the rate to zero. Accordingly, we choose here not to display the mean to first slip.

E. Phase-ramp response

For the phase-ramp input, we provide directly in Fig. 5 the parametric curves established before giving the RMSE-mod as a function of the acquisition time. As before and for a given acquisition time, higher precision can be reached with the RVB estimator compared to the DPLL. Finally, cycle slip metrics are shown in Fig. 6. It clearly appears that using the RVB algorithm instead of a conventional DPLL can lead to a drastic decrease of cycle slip occurrence particularly when σ_ϕ is chosen adequately, i.e., $\sigma_\phi \approx 0.15\pi$ rad and 0.8π rad. In any event, the RVB technique is much less sensitive to the tuning of σ_ϕ than the DPLL is to that of B_L. Finally, note that we have depicted a vertical line that indicates the lowest σ_ϕ where steady-state is reached. Actually, for very small σ_ϕ the innovation term in (20) is not significant enough to compensate for the phase rotation taking place during the estimator update, i.e., for $\sigma_\phi \approx \dot{\phi}_0$ as already observed in [11].

F. Real GNSS data

To finish, we present results using real GNSS data. The latter are collected from a static receiver (USRP X310). Samples are recorded at baseband with a sampling frequency of 4 MHz (2×4 bits per complex sample). To process the signal, we use a GNSS software-based receiver developed by ISAE-SUPAERO. In what follows a single satellite is tracked on its

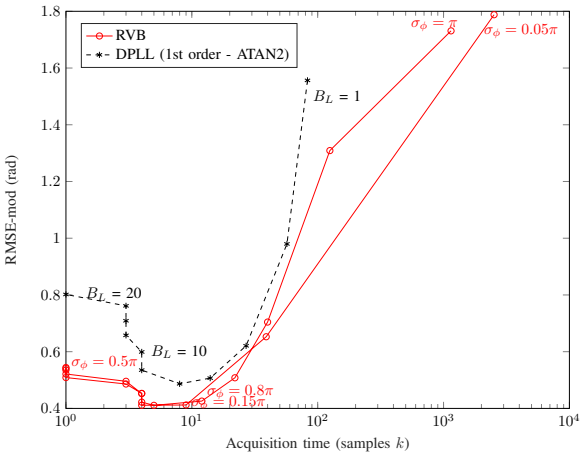

Fig. 5: Precision of estimation metrics comparison for a ramp input: $\dot{\phi}_0 = \pi/30$ rad/sample; σ_n^2 = 1; C/N_0 = 17 dB-Hz.

L1 C/A channel. The tracking architecture chosen is the first solution described in Section II-A, namely we track the prompt phase of a DLL compensated by the frequency estimated at the acquisition stage. Data wipe off is performed too. The correlation time chosen is 1 ms. Phase tracks obtained from the DPLL and the RVB algorithm are depicted for the raw signal in Fig. 7a and with an added synthetic white Gaussian noise in Fig. 7b [7 runs are shown]. The respective C/N_0 are ca. 45 dBHz and 20 dBHz. We may thus consider that tracks from Fig. 7a constitute almost ground truth for that of Fig. 7b. We then clearly see that the DPLL endures systematically a drop-lock beyond ca. 8 seconds whereas the RVB tracks do not show any cycle slip. Another typical behavior of the RVB, can be seen from the zoom in Fig. 7b. If the initial phase is near half a cycle, then the initial RVB estimate (19) may choose one ambiguity range rather than the other in which case a cycle slip does not really occur. Note also from the zoom in Fig. 7a that the RVB converges more rapidly than the DPLL with the values chosen for the processing parameters, namely $\sigma_\phi = 0.8\pi$ rad and $B_L = 10$ Hz. Both have been selected experimentally to provide a low cycle slip occurrence. Finally, it is worth noticing that the RVB performs quite well knowing that its parameters α and σ_n^2 in (5) are estimated via an ad-hoc procedure in practice.

V. Conclusion

Carrier phase measurements are essential for an accurate GNSS-based user positioning. Though, the cycle slip phenomenon has an adverse effect on phase tracking. To obtain a robusitifed phase tracking technique compared to conventional PLL-based approaches, the RVB estimator is proposed. It uses a variational Bayes approximation in the optimal Bayesian filtering problem. The latter preserves the nonlinear nature of the measurement equation which is beneficial at low signal-to-noise ratio towards cycle slipping. Closed-form and easy-to-implement expressions are obtained for the RVB phase estimator. Simulations using synthetic data show that the proposed method offers improvement for both slow phase dynamics considered (viz step and ramp phase inputs) with respect to the cycle slip phenomenon. Finally, the two techniques are compared using real GNSS data at low C/N_0; RVB still outperforms the DPLL in terms of cycle slip occurrence.

References

[1] A. Leick, L. Rapoport, and D. Tatarnikov, *GPS satellite surveying*. John Wiley & Sons, 2015.

[2] B. Hofmann-Wellenhof, H. Lichtenegger, and E. Wasle, *GNSS - Global Navigation Satellite Systems: GPS, GLONASS, Galileo, and more*. Springer Science & Business Media, 2007.

[3] E. Kaplan and C. Hegarty, *Understanding GPS: principles and applications*. Artech house, 2005.

[4] B. Hofmann-Wellenhof, H. Lichtenegger, and J. Collins, *Global positioning system: theory and practice*. Springer Science & Business Media, 2012.

[5] F. J. Charles and W. C. Lindsey, "Some analytical and experimental phase-locked loop results for low signal-to-noise ratios," *Proceedings of the IEEE*, vol. 54, no. 9, pp. 1152–1166, Sep. 1966.

[6] A. J. Viterbi, "Phase-locked loop dynamics in the presence of noise by Fokker-Planck techniques," in *The Foundations Of The Digital Wireless World: Selected Works of AJ Viterbi*. World Scientific, 2010, pp. 13–29.

[7] W. C. Lindsey and C. M. Chie, "A survey of digital phase-locked loops," *Proceedings of the IEEE*, vol. 69, no. 4, pp. 410–431, April 1981.

[8] S. Brunt, M. Darnell, and M. Grayson, "Cycle-slipping probability of first-order phase-locked loop using transient analysis," *IEEE Proceedings-Communications*, vol. 144, no. 5, pp. 357–360, 1997.

[9] J. A. Lopez-Salcedo, J. A. D. Peral-Rosado, and G. Seco-Granados, "Survey on robust carrier tracking techniques," *IEEE Communications Surveys Tutorials*, vol. 16, no. 2, pp. 670–688, Second 2014.

[10] V. Smidl and A. Quinn, "Variational bayesian filtering," *IEEE Transactions on Signal Processing*, vol. 56, no. 10, pp. 5020–5030, 2008.

[11] S. Bidon and S. Roche, "Variational bayes phase tracking for correlated dual-frequency measurements with slow dynamics," *Signal Processing*, vol. 113, pp. 182–194, 2015.

[12] A. V. Oppenheim, R. W. Schafer, and J. R. Buck, *Discrete-time Signal Processing (2Nd Ed.)*. Upper Saddle River, NJ, USA: Prentice-Hall, Inc., 1999.

[13] J. M. N. Leitao and M. A. T. Figueiredo, "Absolute phase image reconstruction: a stochastic nonlinear filtering approach," *IEEE Transactions on Image Processing*, vol. 7, no. 6, pp. 868–882, June 1998.

[14] J.-F. Giovannelli, J. Idier, R. Boubertakh, and A. Herment, "Unsupervised frequency tracking beyond the nyquist frequency using markov chains," *IEEE Transactions on signal processing*, vol. 50, no. 12, pp. 2905–2914, 2002.

[15] R. F. Barrett and D. A. Holdsworth, "Frequency tracking using hidden markov models with amplitude and phase information," *IEEE Transactions on Signal Processing*, vol. 41, no. 10, pp. 2965–2976, Oct 1993.

[16] B. Ristic, S. Arulampalam, and N. Gordon, *Beyond the Kalman filter: Particle filters for tracking applications*. Artech house, 2003.

[17] S. A. Stephens and J. B. Thomas, "Controlled-root formulation for digital phase-locked loops," *IEEE Transactions on Aerospace and Electronic Systems*, vol. 31, no. 1, pp. 78–95, Jan 1995.

[18] F. M. Gardner, *Phaselock techniques*. John Wiley & Sons, 2005.

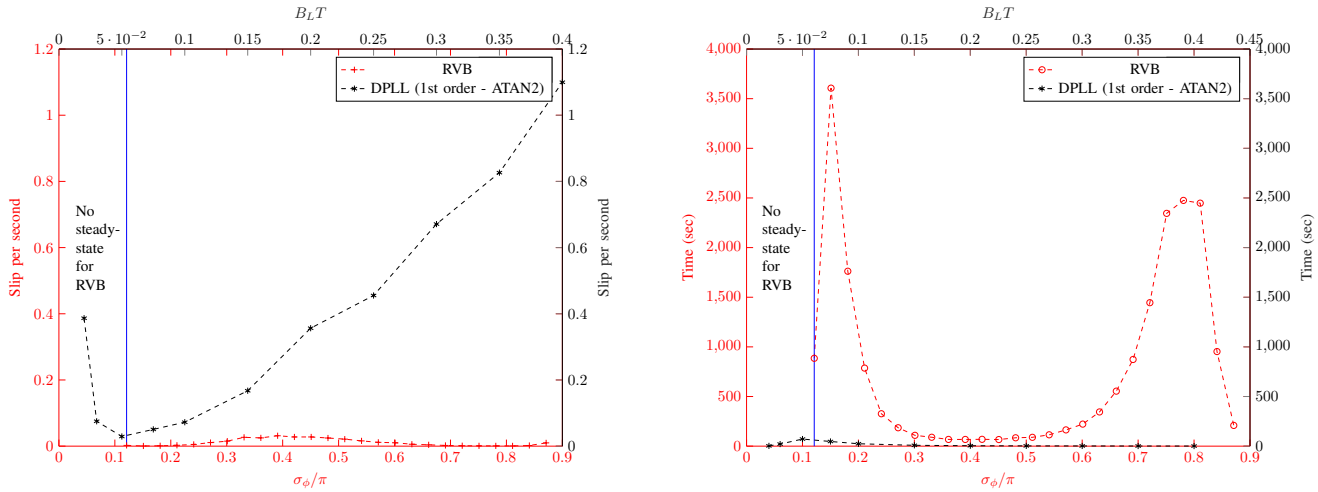

(a) Cycle slip rate

(b) Mean time to first cycle slip

Fig. 6: Cycle slip metrics for a ramp phase input: $\dot{\phi}_0 = \pi/30$ rad/sample; σ_n^2 = 1; C/N_0 = 15 dB-Hz.

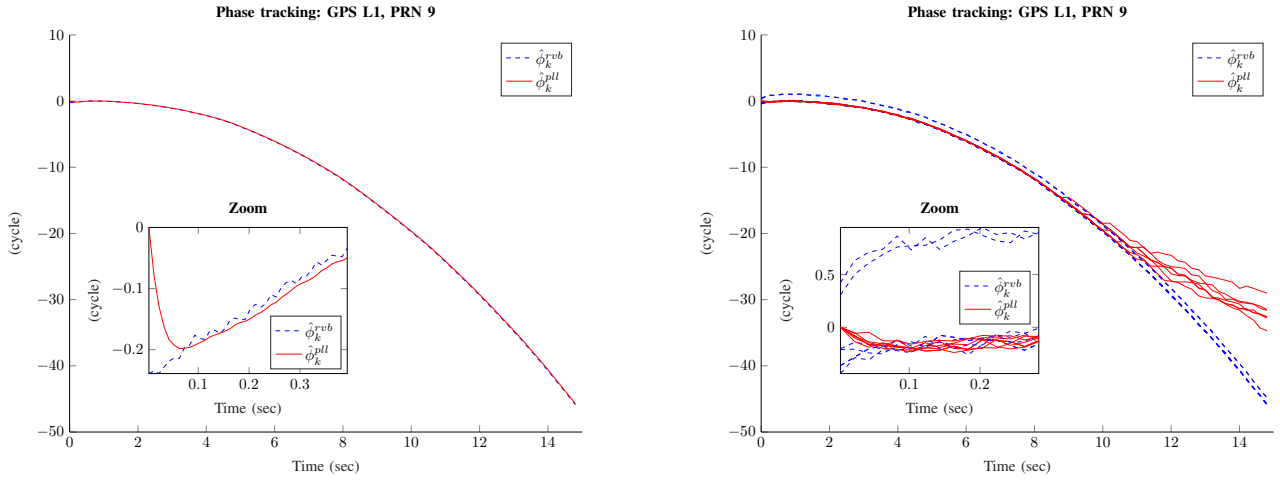

(a) Phase tracking at C/N_0 around 45 dB-Hz

(b) Phase tracking at C/N_0 around 20 dB-Hz

Fig. 7: Phase estimation using real GNSS data; $T = 1$ ms; $f_s = 4$ MHz; Satellite PRN 9; 1) RVB: $\sigma_\phi = 0.8\pi$ rad; $q_{max} = 50$; 2) DPLL: $B_L = 10$ Hz.